Surface Review and Letters, Vol. 9, No. 2 (2002) 1275–1280

THREE-DIMENSIONAL BAND MAPPING BY COMBINED VERY-LOW-ENERGY ELECTRON DIFFRACTION AND PHOTOEMISSION

V. N. STROCOV,*†‡ R. CLAESSEN,* H. I. STARNBERG† and P. O. NILSSON†
*Experimentalphysik II, Universität Augsburg, D-86135 Augsburg, Germany
†Department of Physics, Chalmers University of Technology and Göteborg University, SE-41296 Göteborg, Sweden

G. NICOLAY and S. HÜFNER
Fachrichtung Experimentalphysik, Universität des Saarlandes, D-66041 Saarbrücken, Germany

P. BLAHA
Institute für Physikalische und Theoretische Chemie, Technische Universität Wien, A-1060 Wien, Austria

A. KIMURA, A. HARASAWA, S. SHIN and A. KAKIZAKI
Institute for Solid State Physics, University of Tokyo, Kashiwa, Chiba 277-8581, Japan

Resolving the 3D wave vector $\mathbf{k}$ in photoemission mapping of the band structure $E(\mathbf{k})$ requires knowledge of the unoccupied final states. Both dispersions and lifetimes of these states can be achieved by very-low-energy electron diffraction (VLEED). By incorporating the non-free-electron and excited-state effects in the final states, combining VLEED with photoemission provides accurate mapping of the valence $E(\mathbf{k})$ resolved in the 3D wave vector and under control of the intrinsic accuracy. We here concentrate on the most accurate combined method which uses angle-dependent VLEED and photoemission measurements. It provides access to many Brillouin-zone lines using one crystal surface, and benefits from an intensity gain and a better intrinsic accuracy near the Fermi level.

1. Introduction

Angle-resolved photoemission (PE) spectroscopy[1] is the principal tool for studying the $E(\mathbf{k})$ electronic band structure. Determination of the 3D wave vector $\mathbf{k}$ is based on its conservation in the photoexcitation in the bulk of the crystal. As the photoelectron passes the surface, the surface-parallel component $\mathbf{k}_\parallel$ is conserved, but the surface-perpendicular component $k_\perp$ is distorted. Control over $k_\perp$ (and thus over full $\mathbf{k}$) can be achieved only if the $k_\perp$-dispersions of the PE final states (unoccupied states above the vacuum level $E_{\rm vac}$) are known. Commonly, they are approximated within an empirical free-electron-like (FE-like) model. However, in many cases the final states strongly deviate from this model by non-parabolic dispersions and complicated excited-state self-energy effects.

Only recently has it been demonstrated that the PE-final-state dispersions and, moreover, lifetimes can be directly determined by very-low-energy electron diffraction (VLEED).[3–5] This is based on the fact that the PE final states are related to the LEED states by time reversal.[2] The VLEED energy range of $\sim$ 40 eV above $E_{\rm vac}$ fits the typical final-state energies in PE band mapping. Use of the VLEED experimental final states, incorporating the

‡Also with the Institute for High-Performance Computations and Databases, PO Box 71, 194291 St. Petersburg, Russia.

true non-FE and excited-state effects, in PE band mapping provides accurate determination of the valence $E(\mathbf{k})$ resolved in the 3D wave vector (3D band mapping) and, moreover, under control of the intrinsic accuracy.[4,5] We briefly discuss here the principles of the 3D band mapping by combined VLEED–PE, concentrating on the new most useful method based on angle-dependent measurements.[5]

2. Unoccupied Band Structure by VLEED

The idea of VLEED band determination comes from the matching approach of the LEED theory.[6] The elastic electron reflectivity R (or, more conveniently, transmission $T = 1 - R$) is described by matching of the vacuum-half-space wave function to the crystal-half-space Bloch-wave superposition $\sum_{\mathbf{k}} T_{\mathbf{k}}\phi_{\mathbf{k}}$ under conservation of the incident parallel momentum $\mathbf{K}_{\|}$. The $T(E)$ spectrum is then connected to $E(k_{\perp})$ along the surface-perpendicular direction(s) in the Brillouin zone (BZ) defined by $\mathbf{k}_{\|} = \mathbf{K}_{\|} + \mathbf{g}$. Moreover, it is connected only to those few bands in the $E(k_{\perp})$ manifold which effectively couple to the incident plane wave, taking up significant partial absorbed currents $I_{\mathbf{k}} = |T_{\mathbf{k}}|^2 v_{\perp}$ (v is the group velocity). Whenever the electron energy passes a *critical point* (CP) in the $k_{\perp}$-dispersion of these bands (like the edge of a local band gap), the associated rapid variation of the wave function causes a rapid change in $T(E)$ signaled by an *extremum* in dT/dE (see Fig. 1). Thus the extrema in the VLEED spectrum dT/dE reveal the CPs in the coupling bands of $E(k_{\perp})$. This enables experimental determination of these CPs.[3]

From these experimental points, the full band dispersions in $E(\mathbf{k})$ along the surface-perpendicular directions of the BZ can be determined by fitting the experimental CPs using a semiempirical band calculation.[4,7] Moreover, $E(\mathbf{k})$ along the surface-parallel symmetry lines can be determined from angle-dependent measurements directly by mapping of the experimental CPs along these lines as a function of incidence $\mathbf{K}_{\|}$ (see Fig. 1).[5,3]

The principles of the VLEED band determination can be extended to include finite electron lifetime τ described by the absorption V_i.[7] The Bloch waves all become damped into the crystal with complex $k_{\perp}$. This results in smoothing of the band $k_{\perp}$-dispersions

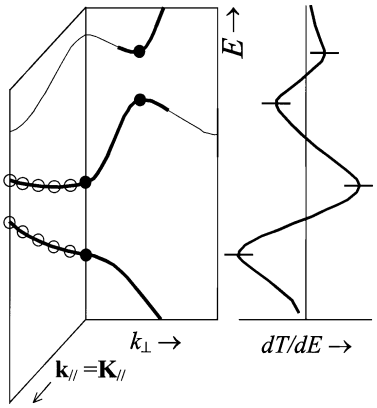

Fig. 1. Principles of VLEED band determination: the critical points in the bands with sufficient coupling to vacuum (filled circles in the bold lines) are reflected by the extrema (dashes) in the VLEED spectrum of the derived elastic transmission dT/dE. Band dispersions along the surface-parallel symmetry lines (open circles) are reflected in the VLEED angle dependencies.

and closing of the band gaps (only $\mathbf{k}_{\|}$ remains real and $\mathbf{k}_{\|}$-dispersions unsmoothed due to surface-parallel invariance of the VLEED process). The CPs become now the points of the extremal (inverse) curvature in $E(\mathrm{Re}k_{\perp})$, which are only slightly shifted from the no-absorption CPs. $I_{\mathbf{k}}$ become the partial electron densities integrated in the crystal half-space $I_{\mathbf{k}} = V_i \int \phi^*_{\mathbf{k}}\phi_{\mathbf{k}} d\mathbf{r}$. These generalizations extend the connection between VLEED and $E(\mathbf{k})$, and thus enable the same band-determination methods.

Besides the band dispersions $E(\mathrm{Re}k_{\perp})$, the above extension allows for accessing the electron lifeimes near the CPs. They can be extracted from broadenings of the VLEED spectral structures.[4] Together with the experimental band-gap widths, the lifetimes give the $\mathrm{Im}k_{\perp}$ values (to the first approximation $\mathrm{Im}k_{\perp} \sim V_i/v_{\perp}$) which determine the final-state broadening in $k_{\perp}$. This information is required to optimize the accuracy of the PE band mapping (see below).

On the practical matters of the VLEED band mapping, its experimental simplicity is remarkable. One can use any inverse-PE or LEED setup operated in the retarding field mode.[8] Although the retarding field distorts the electron trajectories if the sample is rotated for off-symmetry measurements, this problem can be dealt with using electrostatic ray-tracing calculations, or, very effectively, using a parametrized $\mathbf{K}_{\|}$ dependence on energy and the sample rotation with the coefficients fitted to the

experimental points and diffraction patterns with well-defined $\mathbf{K}_{\|}$ values. The VLEED spectra can be measured by the current absorbed by the sample. This technique is referred to as targe (or total) current spectroscopy.[9] Due to excellent signal/noise ratio, the data-acquisition time is usually less than 1 min per spectrum.

It should be noted that in view of a multitude of bands, typical for the unoccupied states, the VLEED-data analysis includes identification of the coupling bands to link the spectral structures with particular CPs (and therefore with particular $k_\perp$). The identification usually employs a semiempirical reference calculation of $E(\mathbf{k})$ and the associated $I_\mathbf{k}$.[5]

Extensive VLEED data obtained on different materials have shown that the unoccupied states, contrary to the common point of view, can be rather complicated. First, they can significantly deviate from an FE-like behavior, especially close to the borders of the BZ. The deviations appear in two aspects: (1) nonparabolic dispersions, whose optimal FE fit $E(\mathbf{k}) = \frac{\hbar^2}{2m^*}(\mathbf{k}+\mathbf{G}) + V_{000}$ yields the effective mass m^* and inner potential V_{000} strongly dependent on energy and $\mathbf{k}$; (2) multiple bands with comparable coupling to vacuum, giving rise to uncertainty in $k_\perp$.[5,7] The non-FE effects are notable even for metals in certain regions in the $\mathbf{k}$-space, as demonstrated below for Cu, and are particularly strong in quasi-2D materials due to strong modulations of the crystal potential. Second, the unoccupied states can contain excited self-energy corrections $\Delta\Sigma$ to the band energies with significant band and $\mathbf{k}$-dependence.[5]

3. 3D Band Mapping by VLEED–PE

3.1. *Principles*

A general connection between VLEED and PE is found within the one-step theory of photoemission:[2] implying the sudden approximation, the photocurrent is determined by $I^{\rm ph} \propto |\langle\Phi_f^*|\mathbf{A}\cdot\mathbf{p}+\mathbf{p}\cdot\mathbf{A}|\Phi_i\rangle|^2$, where Φ_i is the initial-state wave function, $\mathbf{A}$ the vector potential of the screened electric field, $\mathbf{p}$ the momentum operator, and the final-state wave function Φ_f is the time-reversed LEED state. Moreover, the partial photocurrents $I^{\rm ph}_\mathbf{k}$ from different final-state bands are proportional to the currents $I_\mathbf{k}$ absorbed in these bands in VLEED: $I^{\rm ph}_\mathbf{k} = I_\mathbf{k}\cdot(\frac{1}{V_i}\frac{\partial k^i_\perp}{\partial E}|M^{\rm fi}_\mathbf{k}|^2)$, where $M^{\rm fi}_\mathbf{k}$ is the photoexcitation matrix element.[7] Therefore, the dispersions of the coupling bands found in the VLEED experiment can be immediately used for the dominant final bands in PE mapping of the valence bands. Such a combined VLEED–PE approach, naturally incorporating the true non-FE and excited-state self-energy effects in the final bands, enables accurate 3D band mapping.

Knowledge of only the final-state dispersions is not sufficient for accurate 3D band mapping. The final state is damped in the surface-perpendicular direction by finite electron lifetime and elastic scattering off the crystal potential. The corresponding $\mathrm{Im}k_\perp$ gives then its broadening in $k_\perp$. The PE peak is formed by an integration of the valence-band dispersion within this broadening. In this context $\mathrm{Im}k_\perp$ is the *intrinsic* $k_\perp$-resolution of the PE experiment, which cannot be improved instrumentally.[5,10,11] Nonlinearity of the valence-band dispersion or variations of the matrix element within the $k_\perp$-broadening will then give rise to an asymmetry of the PE beak and its intrinsic shift from the true quasiparticle band energy as dictated by the direct transition.[4,5,11] For example, Fig. 2 illustrates the effect of nonlinearity by a model PE calculation for the *sp*-band of Cu approximated by a quadratic dispersion; degrading of the $k_\perp$-resolution results in large intrinsic shifts. Accurate band mapping requires that broadening in $k_\perp$ remain much smaller than the perpendicular dimension of the BZ: $\mathrm{Im}k_\perp \le k_\perp^{\rm BZ}$. Knowledge of the $\mathrm{Im}k_\perp$ from the VLEED experiment can be immediately used to select the final-state energies optimizing the intrinsic accuracy of the PE experiment. In this context an additional advantage of the

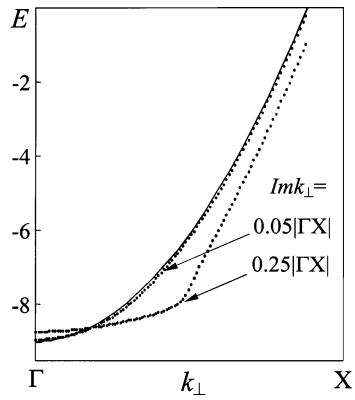

Fig. 2. Model PE experiment for the *sp*-band of Cu approximated by quadratic dispersion. The dots show the peak positions for two final-state $\mathrm{Im}k_\perp$ values determining the $k_\perp$-resolution.

combined VLEED–PE band mapping is the possibility of using low final-state energies, where the FE approximation is inappropriate, to achieve maximal escape-length limited $k_\perp$-resolution and instrumentally limited $\mathbf{k}_\parallel$-resolution.

Reflecting the VLEED band determination by fitting in $E(k_\perp)$ and direct mapping in $E(\mathbf{k}_\parallel)$, the VLEED–PE band mapping can be performed by two methods.

VLEED–PE band mapping in $E(k_\perp)$ is performed varying $k_\perp$ at fixed $\mathbf{K}_\parallel$. This conventional method of 3D band mapping has recently been demonstrated on typical transition metal dichalcigenides VSe_2 and TiS_2.[4] As a consequence of the quasi-2D nature of these materials, the final bands are characterized by very strong non-FE effects. Taking them into account using VLEED was the key point to achieve consistent mapping of the valence bands. Moreover, the region of accurate band mapping was restricted to the final-state energies not exceeding the bulk plasmon excitation threshold: for larger energies the electron lifetime sharply decreased, resulting in degradation of the $k_\perp$-resolution and large intrinsic shifts. The details can be found in Ref. 4.

VLEED–PE band mapping in $E(\mathbf{k}_\parallel)$, or the angle-dependent VLEED-constant-final-state PE (VLEED–CFSPE) method,[5] is performed varying $\mathbf{K}_\parallel$ with $k_\perp$ fixed on a surface-parallel symmetry line of the BZ. While the first method contained fitting schemes, this one is direct. First, one applies the VLEED band mapping to determine $\mathbf{K}_\parallel$-dispersion of a final-state band gap placed on a surface-parallel symmetry line; see Fig. 1. Taking into account the lifetime smoothing of the band dispersions, $k_\perp$ is fixed on this line at the energy in the middle of the gap. $\mathbf{k}$ is then fixed three-dimensionally. Second, one performs PE measurements in the CFS mode with the final-state energy for each $\mathbf{K}_\parallel$ chosen to follow the middle of the gap. $k_\perp$ is thus pinned on the chosen symmetry line, and the PE peaks as a function of $\mathbf{K}_\parallel$ directly yield the valence-band dispersion along this line.

We illustrate below the VLEED–CFSPE method on Cu. Band structure of this material is well documented,[12] which has allowed exhaustive testing of the method. We used the (110) surface which gives access to the whole surface-parallel symmetry plane Γ KLUX. For details see Ref. 5.

3.2. *VLEED–CFSPE method: testing on Cu*

Experimental angle-dependent data on the final states, obtained by VLEED, are shown in Fig. 3 (*upper panel*) rendered into a $\mathbf{K}_\parallel$-dispersion map of the dT/dE spectra. The shading shows the spectral regions from the dT/dE maxima to the nearest minima higher in energy, which are identified by $\frac{d}{dE}(dT/dE) < 0$. The positions of the extrema themselves are shown by bars. This map is basically a direct image of the *surface-projected* $E(\mathbf{k})$ of the unoccupied bands with sufficient coupling to vacuum: as is clear from Fig. 1, the shading shows the interiors of the bands surface-projected out of $E(k_\perp)$, and the points are the CPs of these bands. To identify in the experimental data the band gaps, which correspond to the required surface-parallel symmetry

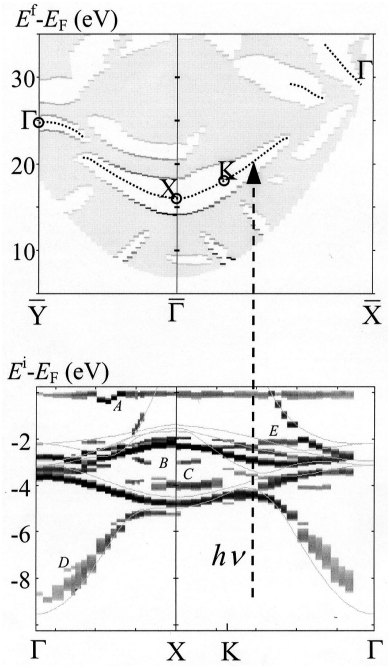

Fig. 3. Electronic structure of Cu. *Upper panel*: VLEED experimental $E(\mathbf{k}_\parallel)$ of the unoccupied coupling bands as the dT/dE extrema connected by maxima-to-minima shading. The extrema are shown in $|\frac{d^2}{dE^2}(dT/dE)|$ gray scale ($\sim$ accuracy). The dotted lines show the final-state energies to place $\mathbf{k}$ on the indicated symmetry lines. *Lower panel*: PE experimental valence band as $-\frac{d^2I}{dE^2} > 0$ (in logarithmic gray scale), reflecting the position and width of the PE peaks. The structures at E_F are due to the Fermi edge, and A–F due to surface states, 1D-DOS, and multiple final bands. The DFT $E(\mathbf{k})$ is also shown. The deviations manifest the excited-state self-energy effects.

lines, we used a model pseudopotential calculation. These gaps give the final-state energies E_{CFS} for the PE experiment (dotted lines). Note discontinuities of the E_{CFS} dispersion, revealing extended regions of strong non-FE effects.

The PE angle-dependent data, measured according to the E_{CFS} dispersion, are shown in Fig. 3 (*lower panel*) rendered into a $\mathbf{K}_{\parallel}$-dispersion map of the negative second derivative $-\frac{d^2I}{dE^2}$ with clipped negative values. Physically, the $-\frac{d^2I}{dE^2}$ maxima locate the position of the PE peaks, including the shoulder-like ones, and thus reflect the band dispersions. This map is therefore the direct image of the valence $E(\mathbf{k})$ along the indicated symmetry lines with $\mathbf{k}$ fixed three-dimensionally.

Our experimental data show excellent internal consistency: the valence bands disperse smoothly even where E_{CFS} has discontinuities. Moreover, it is in perfect agreement with all published experimental data.[12] The valence bands are easily identified by comparison to a band calculation also shown in Fig. 3 (the regular deviations manifest the self-energy effects discussed below).

Intrinsic accuracy of the VLEED–CFSPE method is not significantly limited by some increase of $\mathrm{Im}k_{\perp}$ in the final-state band gaps, which is usually smaller than the lifetime effect. Moreover, as the method may be applied at low final-state energies with large lifetime, on the whole $\mathrm{Im}k_{\perp}$ remains even smaller compared to the conventional method. Due to probing of the dispersion extremum, the VLEED–CFSPE method benefits from vanishing peak width for the electron-like bands near the Fermi surface.

Practical advantages of the VLEED–CFSPE method are remarkable. First, this method is direct. Second, it allows for accessing a variety of BZ directions through one crystal surface. Indeed, the experimental data in Fig. 3 cover almost the whole body of the previous data[12] and deliver completely new pieces of $E(\mathbf{k})$ like the *sp*-band along the whole ΓX line. It has therefore no alternatives for the materials with only one stable surface, like the layered materials. Third, by probing the valence states in their maximal 1DOS the method benefits from an intensity gain. Finally, being a truly 3D band-mapping method, the angle-dependent VLEED–PE method naturally incorporates the non-FE and excited-state effects in the final bands. Exhaustively tested on Cu, it is most useful for non-FE materials.

3.3. *Electronic structure of Cu*

Our experimental results show some less expected properties of the electronic structure of Cu. First, the VLEED results show significant deviations of the final bands from an FE-like behavior. This is clearly seen in the $\mathbf{K}_{\parallel}$-dispersion map in Fig. 3: the dispersions show large band gaps and, moreover, closer to the borders of the BZ the dispersions become nonparabolic and even undergo discontinuities. This reveals extended regions of strong band hybridization. The $k_{\perp}$-dispersions in these regions, although smoothed by finite lifetime, go nearly vertically. This behavior was confirmed by PE, measuring a constant-$\mathbf{k}_{\parallel}$ series of CFS spectra with the final-state energies going through these regions.

Second, the experimental valence band regularly and significantly deviates from the DFT band structure also shown in Fig. 3. Our calculation used the GGA exchange correlation (the differences from the LDA were negligible) and was performed with the FLAPW code WIEN97.[13] The whole *d*-band manifold is ~ 0.5 eV lower than calculated and the *sp*-band in its bottom ~ 0.5 eV higher. Any significant experimental or computational errors can be ruled out, because our results are in excellent agreement with all other experimental data and state-of-the art DFT calculations. In fact, the deviations reflect self-energy corrections $\Delta\mathrm{Re}\Sigma$ due to difference of the excited-state exchange correlation, described by the self-energy operator, from the ground-state DFT one. They are connected with spatial localization of the wave function.[14] Moreover, the unoccupied bands demonstrate the same behavior. It is intriguing to find so pronounced self-energy effects in the weakly correlated Cu metal. They are, however, well reproduced by a quasiparticle GW calculation. A detailed analysis will be presented elsewhere.

4. Conclusion

We have demonstrated that the combination of VLEED and PE provides a powerful tool for truly 3D band mapping. It is based on independent determination of the PE final states by VLEED. The main advantage of this combination is natural incorporation of the non-FE dispersions, excited-state self-energy corrections and lifetimes in the final states. In particular, knowledge of the lifetimes enables control over the intrinsic accuracy of the PE experiment

determined by the final-state **k**-broadening. We have described details of the new angle-dependent VLEED–PE method employing emission out of the final-state band gaps placed on the surface-parallel lines of the BZ. Besides being direct, the method benefits from accessing many BZ lines using one crystal surface, intensity gain, and better intrinsic accuracy near the Fermi level.

References

1. *Angle-Resolved Photoemission*, ed. S. D. Kevan (Elsevier, Amsterdam, 1992); S. Hüfner, *Photoelectron Spectroscopy* (Springer, Berlin, 1995).
2. P. J. Feibelman and D. E. Eastman, *Phys. Rev.* **B10**, 4932 (1974); J. B. Pendry, *Surf. Sci.* **57**, 679 (1976).
3. V. N. Strocov, *Solid State Commun.* **78**, 545 (1991); *Int. J. Mod. Phys.* **B9**, 1755 (1995).
4. V. N. Strocov *et al.*, *Phys. Rev. Lett.* **79**, 467 (1997); *J. Phys.: Condens. Matter* **10**, 5749 (1998).
5. V. N. Strocov *et al.*, *Phys. Rev. Lett.* **81**, 4943 (1998); *Phys. Rev.* **B63**, 205108 (2001).
6. G. Capart, *Surf. Sci.* **13**, 361 (1969); J. B. Pendry, *Low Energy Electron Diffraction* (Academic, London, 1974).
7. V. N. Strocov, H. Starnberg and P. O. Nilsson, *J. Phys.: Cond. Matter* **8**, 7539 (1996); *Phys. Rev.* **B56**, 1717 (1997).
8. V. N. Strocov, *Meas. Sci. Technol.* **7**, 1636 (1996).
9. S. A. Komolov, *Total Current Spectroscopy of Surfaces* (Gordon and Breach, Philadelphia, 1992).
10. R. Matzdorf, *Appl. Phys.* **A63**, 549 (1996).
11. V. N. Strocov, in *Electron Spectroscopies Applied to Low-Dimensional Materials*, eds. H. I. Starnberg and H. P. Hughes (Kluwer, Netherlands, 2000).
12. R. Courths and S. Hüfner, *Phys. Rep.* **112**, 53 (1984); R. Matzdorf, *Surf. Sci. Rep.* **30**, 153 (1998).
13. P. Blaha, K. Schwarz and J. Luitz, WIEN97, A Full Potential Linearized Augmented Plane Wave Package for Calculating Crystal Properties (Tech. Universität WIEN, Austria, 1999).
14. P. O. Nilsson and C. G. Larsson, *Phys. Rev.* **B27**, 6143 (1983); V. N. Strocov *et al.*, to be published.